Fitoterapia 187 (2025) 106895

Contents lists available at ScienceDirect

Fitoterapia

journal homepage: www.elsevier.com/locate/fitote

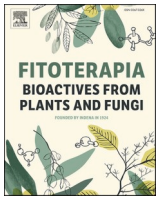

Research Paper

Synergistic effect of plant-derived deglucoruscin in combination with conventional antimicrobials against *Staphylococcus aureus* and *Candida albicans*

Carmen Festa [a], Claudia Finamore [a], Mattia Cammarota [a], Elisabetta Panza [a], Silvia Marchianò [b], Stefano Fiorucci [b], Angela Zampella [a], Elisabetta Buommino [a], Simona De Marino [a,*]

[a] Department of Pharmacy, University of Naples, Via Domenico Montesano, 49, Naples 80131, Italy
[b] Department of Medicine and Surgery, University of Perugia, Piazza L. Severi, 1, Perugia 06132, Italy

ARTICLE INFO

Keywords:
Ruscus aculeatus
Furostanol saponins
Deglucoruscin
NMR spectroscopy
Candida albicans
Synergism

ABSTRACT

A detailed phytochemical investigation of rhizomes and roots of *Ruscus aculeatus* led to the isolation of fifteen pure compounds, belonging to the furostanol and spirostanol glycoside classes. Among them, one novel furostanol saponin (**1**) was identified, alongside twelve known furostanol (**2**–**8**) and spirostanol (**11**–**15**) saponins and two sulphated glycosides (**9**–**10**). Structural elucidation of all isolated compounds was accomplished through comprehensive 1D and 2D NMR spectroscopic analyses, complemented by mass spectrometry. The $CHCl_3$ extract of *Ruscus aculeatus* and its major metabolite, the spirostanol derivative (**12**), exhibited a weak antimicrobial activity. Of particular interest, compound **12** when co-administered with voriconazole (VRC) showed a significant inhibitory effect against the azole-resistant *Candida albicans* ATCC 10231 strain, demonstrating a synergistic effect that underscores its potential to restore antifungal efficacy and combat resistance mechanisms.

These findings highlight compound **12** as a promising adjuvant candidate in antifungal therapy, particularly against resistant *Candida* strains.

1. Introduction

Terrestrial organisms represent an extraordinarily rich source of active secondary metabolites, which often possess complex and unique chemical scaffolds. These molecules are an important resource and models for the development of rationally designed multi-target drugs. Several kinds of plant-derived ingredients have a vast variety of biological activities. Our research focuses on the discovery of natural molecules able to interact with specific pharmacological targets; thus, accordingly, we conducted the isolation of individual secondary metabolites from the hydroalcoholic extract of *Ruscus aculeatus* to identify potential new antimicrobial agents.

Ruscus aculeatus, commonly known as butcher's broom and belonging to the Asparagaceae family, is native to Mediterranean Europe, the northern parts of Africa (Morocco, Algeria, Tunisia, and Libya) and often grow in well-shaded areas such as woodlands, hedgerows, and coastal cliffs [1]. This evergreen shrub typically grows to a height of 60–80 cm and bears distinctive red berries. The stems are rigid and bear spine-tipped triangular leaves which are reduced cladodes. Since the Middle Ages, the underground parts of *Ruscus aculeatus* L., particularly the roots and rhizomes, have been widely used in traditional medicine as phytotherapeutic and phlebotherapeutic agents [2].

Ruscus aculeatus extracts have demonstrated a broad spectrum of biological activities. Among their most well-known traditional applications, the hydroalcoholic extract of rhizomes, has been traditionally used in Europe as a vascular tonic and preventive agent, in the treatment

Abbreviations: AMB, Amphotericin B; CVI, Chronic venous insufficiency; DMSO, Dimethyl sulfoxide; EtOAc, Ethyl acetate; FIC, Fractional Inhibitory Concentration; HMP, 2-hydroxy-3-methylpentanoyl; MIC, Minimal inhibitory concentration; MRSA, *S. aureus* methicillin resistant; MTT, 3-(4,5-di methyl thiazol-2-yl)-2,5-diphenyltetrazolium bromide; NSAID, Non-steroidal antiinflammatory drug; OXA, Oxacillin; TOB, Tobramycin; VAN, Vancomycin; VRC, Voriconazole; WHO, World Health Organization.

* Corresponding author.
E-mail addresses: carmen.festa@unina.it (C. Festa), claudia.finamore@unina.it (C. Finamore), mattia.cammarota@unina.it (M. Cammarota), elisabetta.panza@unina.it (E. Panza), stefano.fiorucci@unipg.it (S. Fiorucci), azampell@unina.it (A. Zampella), elisabetta.buommino@unina.it (E. Buommino), simona.demarino@unina.it (S. De Marino).

https://doi.org/10.1016/j.fitote.2025.106895
Received 30 July 2025; Received in revised form 9 September 2025; Accepted 23 September 2025
Available online 24 September 2025

of venous insufficiency, capillary fragility, and varicose veins [3,4].

Traditional uses include also the treatment of urinary disorders, kidney stones, and abdominal pain [2]. Decoctions prepared from the roots and rhizomes have been recommended for alleviating symptoms such as venous insufficiency, edema, eczema, premenstrual syndrome, inflammation, and hemorrhoids [2,5,6]. Furthermore, extracts have also been used as a preventive of atherosclerosis and circulatory insufficiency [2,6,7].

In 2019, Chakuleska et al. explored for the first time the *in vitro* effects of *R. aculeatus* extracts on the proliferation of human osteoblast-like SaOS-2 cells and on bone structure in estrogen-deficient rats. The results suggest that *R. aculeatus* extracts could be promising candidates for the prevention of postmenopausal osteoporosis [7].

The antioxidant properties of *R. aculeatus* extracts have been attributed in part to the presence of phenolic compounds such as p-coumaric acid, caffeic acid, and rutin. Additionally, crude steroidal saponin mixtures extracted from the rhizomes have demonstrated a notable anti-inflammatory effect. In some cases, this activity was even more pronounced than that of the reference non-steroidal anti-inflammatory drug (NSAID), diclofenac (20 mg/kg). The underlying mechanism appears to involve the inhibition of prostaglandin synthesis, similar to conventional NSAIDs [8].

The antibacterial activity of *Ruscus* extracts and their isolated compounds was also evaluated, with the ethyl acetate (EtOAc) fraction of aerial parts showing the highest efficacy. Among the isolated compounds, rutin, p-coumaric acid, and caffeic acid showed notable antibacterial effects. Both the EtOAc fraction and rutin exhibited bacteriostatic activity against *Staphylococcus aureus* comparable to standard antibiotics, while rutin and p-coumaric acid demonstrated bactericidal activity against *Escherichia coli*, *Pseudomonas aeruginosa*, *Salmonella typhimurium*, and *Enterobacter cloacae* [9]. Notably, *Ruscus aculeatus* extracts have demonstrated significant antifungal activity, with activity in some cases exceeding that of conventional drugs such as streptomycin, ampicillin, bifonazole, and ketoconazole [10].

Considering the rise of antimicrobial resistance, a critical challenge in modern medicine represents the discovery of novel therapeutic strategies. One of the most promising approaches is the use of combination therapy, where a natural compound that may have weak activity on its own can synergistically enhance the efficacy of a conventional drug, overcoming resistance and reducing required dosages.

As part of our ongoing interest in identifying potential new bioactive molecules from plants [10,11], we studied the hydroalcoholic extract obtained from rhizomes and roots of *Ruscus aculeatus*, to determine its secondary metabolite profile and, more importantly, to investigate the potential of its isolated compounds to act as synergistic partners for voriconazole against *Candida albicans* and oxacillin against *Staphylococcus aureus*. These studies led to the identification of deglucoruscin, a spirostanol saponin, previously isolated from *Ruscus aculeatus,* which acts as a synergistic agent when combined with known antimicrobial drugs.

2. Materials and methods

2.1. General experimental procedures

ESI-MS spectra were performed on a mass spectrometer LTQ-XL.

NMR spectra were obtained on a Bruker Avance NEO 400 spectrometer (400 and 700 MHz for ^{1}H, 100 and 175 MHz for ^{13}C, respectively), recorded in CD_3OD ($\delta_H = 3.31$ and $\delta_C = 49.0$ ppm). *J* are in Hz, and chemical shifts (δ) are reported in ppm and referred to CHD_2OD as internal standard; multiplicities are given as s (singlet), br s (broad singlet), d (doublet), dd (double doublet) or m (multiplet) and the coupling constants *J* are in Hz.

Droplet counter current chromatography (DCCC) was carried out using a DCC-A apparatus (Tokyo Rikakikai Co., Tokyo, Japan) equipped with 250 glass-columns (internal diameter 3 mm).

Table 1
NMR spectral data (CD_3OD, 700 MHz) of compound **1.**

	Aglycone mojety			Sugar portion	
				α-L-Ara	
position	δ_H	δ_C	position	δ_H	δ_C
1	3.39 ovl	84.1	1	4.33 d (7.7)	100.5
2	2.09 m, 1.69 m	36.9	2	3.71 dd (9.4, 7.7)	75.3
3	3.35 ovl	69.2	3	3.84 dd (9.4, 3.6)	74.3
4	2.20 m	43.4	4	5.02 m	74.1
5	–	139.4	5	3.88 ovl, 3.57 d (12.9)	64.6
6	5.56 br d (5.7)	125.5		**α-L-Rha**	
7	1.97 m, 1.51 ovl	32.7	1	5.29 br d (1.3)	101.1
8	1.55 ovl	34.1	2	3.88 ovl	72.1
9	1.25 ovl	51.2	3	3.68 dd (9.3, 3.2)	71.9
10		43.2	4	3.40 ovl	73.9
11	2.56 m, 1.49 ovl	24.8	5	4.08 m	69.5
12	1.65 m, 1.20 m	41.0	6	1.25 d (6.1)	18.0
13	–	43.7		**β-D-Glc**	
14	1.04 ovl	56.2	1	4.27 d (7.8)	102.6
15	–		2	3.21 t (9.0)	74.9
16	4.70 m	85.7	3	3.34 ovl	77.9
17	2.49 d (10.1)	65.6	4	3.29 t (9.0)	71.5
18	0.72 s	14.4	5	3.25 m	77.7
19	1.10 s	14.6	6	3.87 ovl, 3.66 d (12.0)	62.6
20	–	105.2		**HMP**	
21	1.61 s	11.4	1	–	179.8
22	–	152.1	2	4.07 d (12.8)	76.4
23	2.27 m	25.0	3	1.88 m	40.1
24	2.26 m	31.3	4	1.64 m, 1.30 m	25.0
25	–	146.3	5	0.95 t (7.5)	11.5
26	4.33 d (12.6), 4.11 d (12.6)	72.7	6	1.01 d (6.8)	15.3
27	5.09 br s, 4.93 br s	112.3			

Coupling constants in parentheses (*J* in Hz); ^{1}H and ^{13}C assignments aided by ^{1}H—^{1}H COSY, HSQC, and HMBC experiments. Ovl: overlapped with other signals; HMP = 2-hydroxy-3-methylpentanoyl mojety.

HPLC was performed using a Waters 510 pump equipped with Waters Rheodyne injector and a Waters 401 differential refractometer as detector, using a reverse phase Nucleodur 100–5 C18 column (5 μm; 4.6 mm i.d. x 250 mm; flow rate 1 mL/min), eluting in isocratic mode with different MeOH/H_2O mixtures. The purity of all compounds was determined to be greater than 95 % by HPLC, MS and NMR.

The GC/MS analysis was carried out with an Agilent Technologies 6890 N gas chromatograph coupled to an Agilent Technologies 5973 N quadrupole mass selective spectrometer and provided with a split/splitless injection port. Helium was used as carrier gas at a linear velocity of 40 cm/s.

Specific rotations were measured on a Perkin Elmer 343B polarimeter.

2.2. Plant material

Indena, the leading company dedicated to the identification and production of active principles derived from plants for use in the pharmaceutical and health food industries, has provided us the hydroalcoholic extract obtained from rhizomes and roots of *Ruscus aculeatus.*

2.3. Extraction and isolation

A modified Kupchan partitioning procedure [12] afforded three extracts: *n*-hexane, $CHCl_3$, and *n*-BuOH. Subsequent purification of the $CHCl_3$ and *n*-BuOH extracts resulted in the isolation of a new furostanol saponin (**1**), twelve known furostanol and spirostanol saponins (**2**–**8**, **11**–**15**), and two sulphated glycosides (**9, 10**) (Tables S1 and S2).

*2.3.1. Acid hydrolysis of deglucoruscin **12** to obtain the aglycone neoruscogenin **(12a)***

Deglucoruscin (20 mg) was hydrolysed with 2 N H_2SO_4 (2 mL) at reflux for 2 h. After cooling, the solution was diluted with $NaHCO_3$ satured solution (5 mL) and extracted with AcOEt (3 × 2 mL). The organic layer was evaporated to dryness under reduced pressure and the residue was purified with HPLC using MeOH/H_2O (88:12) as eluent to give 3.4 mg of neoruscogenin (**12a**) (t_R 17.6 min).

*2.3.2. Characteristic data for Neoruscogenin **(12a)***

Selected ^{1}H NMR (400 MHz, CD_3OD): δ_H 5.55 (1H, br d, J = 5.2 Hz, H-6), 4.77 (1H, br s, H-27a), 4.74 (1H, br s, H-27b), 4.45 (1H, m, H-16), 4.27 (1H, d, J = 12.3 Hz), 3.82 (1H, d, J = 12.3 Hz), 3.41 (2H, m, H-3, H-6), 1.04 (3H, s, H_3–19), 0.94 (3H, d, J = 6.9 Hz, H_3–21), 0.84 (3H, s, H_3–18). ^{13}C NMR (100 MHz, CD_3OD): δ_C 145.2, 140.1, 125.8, 110.7, 108.9, 82.5, 78.9, 68.9, 65.8, 64.1, 57.9, 52.1, 44.1, 43.2, 42.8, 42.4, 41.3, 41.1, 34.0, 33.9, 32.9 (2C), 29.5, 24.8, 16.9, 14.9, 13.8.

*2.3.3. 26-O-β-D-glucopyranosyl-furosta-5,20(22),25(27)-triene-1β,3β,26-triol 1-O-α-L-rhamnopyranosyl-(1 → 2)-4-[(2S,3S)-2-hydroxy-3-methylpentanoyl]-α-L-arabinopyranoside **(1)***

Amorphous solid. $[\alpha]_D^{25}$ − 16.4 (*c* 0.05, MeOH); ESI-MS *m/z* 1005.5 $[M + Na]^+$. The ^{1}H and ^{13}C NMR spectral data are listed in Table 1.

*2.3.4. Sugar analysis for compound **1***

Compound **1** (0.5 mg) was dissolved in anhydrous 2 N HCl-MeOH (0.5 mL) and heated at 80 °C in a stoppered reaction vial. After 2 h, the reaction mixture was cooled, neutralized with Ag_2CO_3, and centrifuged. The supernatant was taken to dryness under a stream of N_2. The residue was reacted with 0.1 M L-cysteine methyl ester hydrochloride in anhydrous pyridine (200 mL) for 2 h at 80 °C. 1-(Trimethylsilyl)imidazole in pyridine was added and the thiazolidine derivatives analyzed by GC–MS. L-Rhamnose, L-arabinose and D-glucose were confirmed in 1 by comparison of the retention times of their derivatives with those of standards.

*2.3.5. 26-O-β-D-glucopyranosylfurosta-5,20(22),25(27)-triene-lβ,3β,26-triol 1-O-{O-α-L-rhamnopyranosyl-(1 → 2)-α-L-arabinopyranoside}**(2)***

Amorphous solid. $[\alpha]_D^{25}$ − 19.7 (c 0.08, MeOH); ESI-MS *m/z* 891.4 $[M + Na]^+$. The ^{1}H and ^{13}C NMR spectral data are consistent with the published data [13].

*2.3.6. 26-O-β-D-glucopyranosyl-22-O-methylfurosta-5,25(27)-diene-1β,3β,22ε,26-tetrol 1-O-{O-α-L-rhamnopyranosyl-(1 → 2)-3-O-acetyl-4-O-[(2S,3S)-2-hydroxy-3-methylpentanoyl]-α-L-arabinopyranoside} **(3)***

Amorphous solid. $[\alpha]_D^{25}$ − 17.8 (*c* 0.10, MeOH); ESI-MS *m/z* 1023.5 $[M - H]^-$. The ^{1}H and ^{13}C NMR spectral data are consistent with the published data [14].

*2.3.7. 1-O-[α-L-rhamnopyranosyl-(1 → 2)-α-L-arabinopyranosyl (1)]-1β, 3β, 22α, 26-tetrahydroxy-furosta-5(6), 25(27)-dien-26-β D-glucopyranoside or Ruscoponticoside E **(4)***

Amorphous solid. $[\alpha]_D^{25}$ − 30.5 (*c* 0.15, MeOH); ESI-MS *m/z* 909.4 $[M + Na]^+$. The ^{1}H and ^{13}C NMR spectral data are consistent with the published data [15].

*2.3.8. 1-O-[β-D-glucopyranosyl-(1 → 3)-α-L-rhamnopyranosyl-(1 → 2)-α-L-arabinopyranosyl (1)]-1β, 3β, 22α, 26-tetrahydroxy-furosta-5(6), 25 (27)-dien-26-β D-glucopyranoside or Ruscoside **(5)***

Amorphous solid. $[\alpha]_D^{25}$ − 30.7 (*c* 0.28, MeOH); ESI-MS *m/z* 1071.5 $[M + Na]^+$. The ^{1}H and ^{13}C NMR spectral data are consistent with the published data [16,17].

*2.3.9. 26-O-β-D-glucopyranosyl-22-O-methyl-furosta-5,25(27)-diene-1β,3β,22α,26-tetrol 1-O-[α-L-rhamnopyranosyl-(1 → 2)-α-L-arabinopyranoside] **(6)***

Amorphous solid. $[\alpha]_D^{25}$ − 33.1 (*c* 0.27, MeOH); ESI-MS *m/z* 923.5 $[M + Na]^+$. The ^{1}H and ^{13}C NMR spectral data are consistent with the published data [18].

*2.3.10. 26-O-β-D-glucopyranosyl-22-O-methyl-furosta-5,25(27)-diene-1β,3β,22α,26-tetrol 1-O-[α-L-rhamnopyranosyl-(1 → 2)-4-O-[(2S,3S)-2-hydroxy-3-methylpentanoyl]-α-L-arabinopyranoside] **(7)***

Amorphous solid. $[\alpha]_D^{25}$ − 32.8 (*c* 0.04, MeOH); ESI-MS *m/z* 1037.5 $[M + Na]^+$. The ^{1}H and ^{13}C NMR spectral data are consistent with the published data [14,19].

*2.3.11. 26-O-β-D-glucopyranosyl-22-O-methyl-furosta-5,25(27)-diene-1β,3β,22α,26-tetrol 1-O-[α-L-rhamnopyranosyl-(1 → 2)-3-O-acetyl-4-O-[(2S,3S)-2-hydroxy-3-methylpentanoyl]-α-L-arabinopyranoside] **(8)***

Amorphous solid. $[\alpha]_D^{25}$ − 27.0 (*c* 0.13, MeOH); ESI-MS *m/z* 1057.6 $[M + H]^+$. The ^{1}H and ^{13}C NMR spectral data are consistent with the published data [14,20].

*2.3.12. (25S)-furost-5,20(22)-diene-1β,3β-diol 1-sulfate 26-O-β-D-glucopyranoside or Nolinofuranoside G). **(9)***

Amorphous solid. $[\alpha]_D^{25}$ − 28.1 (*c* 0.07, MeOH); ESI-MS *m/z* 671.3 $[M - H]^-$. The ^{1}H and ^{13}C NMR spectral data are consistent with the published data [20].

*2.3.13. [(25R),26-O-β-D-glucopyranosyl-22-O-methyl-furost-5-ene-1β,3β,22α,26-tetraol 1-O-sulphate] **(10)***

Amorphous solid. $[\alpha]_D^{25}$ − 29.2 (*c* 0.10, MeOH); ESI-MS *m/z* 703.3 $[M - H]^-$. The ^{1}H and ^{13}C NMR spectral data are consistent with the published data [21].

*2.3.14. 1-O-[α-L-arabinopyranosyl-(1)]spirosta-5(6),25(27)-diene-1β, 3β-diol or Desglucodesrhamnoruscin **(11)***

Amorphous solid. $[\alpha]_D^{25}$ − 37.7 (*c* 0.22, MeOH); ESI-MS *m/z* 583.3 $[M + Na]^+$. The ^{1}H and ^{13}C NMR spectral data are consistent with the published data [22].

*2.3.15. 1-O-[α-L-rhamnopyranosyl-(1 → 2)-α-L-arabinopyranosyl (1)]-spirosta-5(6),25(27)-diene-1β, 3β-diol or Deglucoruscin or Ruscoponticoside C **(12)***

Amorphous solid. $[\alpha]_D^{25}$ − 61.1 (*c* 0.10, MeOH); ESI-MS *m/z* 729.4 $[M + Na]^+$. The ^{1}H and ^{13}C NMR spectral data are consistent with the published data [21,23].

*2.3.16. 4'-O-(2-hydroxy-3-methylpentanoyl)-deglucoruscin **(13)***

Amorphous solid. $[\alpha]_D^{25}$ − 22.3 (*c* 0.10, MeOH); ESI-MS *m/z* 843.4 $[M + Na]^+$. The ^{1}H and ^{13}C NMR spectral data are consistent with the published data [24].

*2.3.17. 1-O-[β-D-glucopyranosyl-(1 → 3)-α-L-rhamnopyranosyl-(1 → 2)-α-L-arabinopyranosyl (1)]-spirosta-5(6), 25(27)-dien-1β, 3β diol or Ruscin or ruscoponticoside D **(14)***

Amorphous solid. $[\alpha]_D^{25}$ − 27.6 (*c* 0.10, MeOH); ESI-MS *m/z* 891.4 $[M + Na]^+$. The ^{1}H and ^{13}C NMR spectral data are consistent with the published data [23].

*2.3.18. [(25R)-3β-hydroxyspitost-5-en-1β-yl O-α-L-rhamnopyranosyl- (1 → 2)-β-D-glucopyranoside] **(15)***

Amorphous solid. $[\alpha]_D^{25}$ − 28.0 (*c* 0.06, MeOH); ESI-MS *m/z* 761.4[M + Na]$^+$. The ^{1}H and ^{13}C NMR spectral data are consistent with the published data [25].

2.4. Antibiotics and strains

Vancomycin and oxacillin were purchased from Sigma-Aldrich (Milan, Italy). *S. aureus* ATCC 29213, *S. aureus* ATCC 43300 *(S. aureus* methicillin resistant - MRSA), *E. coli* ATCC 25922, *C. albicans* ATCC 10231 (an azole resistant strain) were obtained from the American Type Culture Collection (Rockville, MD).

2.5. Antibacterial susceptibility testing

Antimicrobial susceptibility testing Minimal Inhibitory Concentrations (MIC) of the compounds were determined in Mueller–Hinton medium (MH) by the broth microdilution assay, following the procedure already described [27]. The compounds were added to bacterial suspension in each well yielding a final cell concentration of 1×10^6 CFU/mL and a final compound concentration ranging from 16 to 128 μg/mL. Negative control wells were set to contain bacteria in Mueller–Hinton broth plus the amount of vehicle (DMSO) used to dilute each compound. Positive controls included vancomycin (VAN-2 μg/mL) and oxacillin (OXA-2 μg/mL), tobramycin (TOB-2 μg/mL). All antibiotic concentrations reported are according to breakpoint values reported in the EUCAST v.12.0 (The European Committee on Antimicrobial Susceptibility Testing. Breakpoint Tables for Interpretation of MICs and Zone Diameters. Version 12.0, 2022). The MIC was defined as the lowest concentration of the drug that caused a total inhibition of microbial growth after 24 h incubation time at 37 °*C. Medium* turbidity was measured by a microtiter plate reader (Thermo Scientific Multiskan GO, Waltham, MA, United States) at 595 nm. Minimum bactericidal concentration (MBC) was defined as the concentration that caused ≥3log10 reduction in colony count from the starting inoculum plated on TSA, incubated for 24 h at 37 °C.

2.6. Antifungal susceptibility testing

The antifungal activity of compounds was determined on *C. albicans* by using a standardized broth microdilution method (Clinical and Laboratory Standards Institute (CLSI), Performance Standards for Antifungal Susceptibility Testing of Yeasts. third ed. CLSI supplement M27M44S, 2022). Briefly, the cell suspension was adjusted to 3×10^3 CFU/mL in RPMI 1640 medium (Sigma) supplemented with 0.2 % (*w/v*) glucose. One hundred microliter aliquots of these cell suspensions were dispensed into 96-well microtiter plates. Compounds were serially diluted using RPMI1640 medium and added to the wells at a final concentration ranging from 16 to 128 μg/mL, and the plate was incubated for 48 h at 37 °C. Amphotericin B (AMB, 2 μg/mL) and VRC (0.12 μg/mL for *C. albicans* ATCC 10231) were chosen as the positive controls. The minimal inhibitory concentration (MIC) was defined as the lowest concentration of the compound that resulted in 100 % growth inhibition after 24 h of incubation.

2.7. Checkerboard method

The interaction between compound **12** and oxacillin or voriconazole against MRSA and *C. albicans* ATCC10231, respectively, was evaluated by the checkerboard method in 96-well microtiter plates containing the specific broths. Briefly, the tested compounds were serially diluted along the y and x axes, respectively. The final concentration ranged from 0.06 to 32 μg/mL (0.06, 0.12, 0.25, 0.5, 1, 2, 4, 8, 16, 32) for antibiotics and from 4 to 128 μg/mL (4, 8, 16, 32, 64, 128) for compound **12**. The checkerboard plates were inoculated with bacteria at an approximate concentration of $10^5 \times$ CFU/mL, and 3×10^3 CFU/mL for yeasts, and incubated at 37 °C for 24 h (48 h for yeasts), following which microbial growth was assessed visually and the turbidity measured by microplate reader at 595 nm. The FIC index for each combination was calculated as follows: FIC index = FIC of compound **12** + FIC of antibiotics, where FIC of compound **12** (or antibiotics) was defined as the ratio of MIC of **12** (or antibiotics) in combination and MIC of **12** (or antibiotics) alone.

The FIC index values were interpreted as follows: ≤0.5, synergistic; >0.5 to ≤1.0, additive; >1.0 to ≤2.0, indifferent; and > 2.0, antagonistic effects [28].

2.8. Statistical analysis

All the tests were conducted at least three times using independent cell suspensions. Arithmetic means and standard deviations were calculated. Student's *t*-test was used to determine statistical differences between group means. A *p*-value ≤0.05 was indicative of a significant difference.

2.9. MTT assay

Human HaCaT keratinocyte cells, sourced from the American Type Culture Collection (ATCC, Manassas, VA, USA), were cultivated in Dulbecco's Modified Eagle Medium (DMEM; Sigma-Aldrich, Milan, Italy, cat. no. D6546), enriched with 10 % fetal bovine serum (FBS; Gibco, Milan, Italy, cat. no. A4736301), 100 U/mL penicillin and 100 μg/mL streptomycin (cat. no. 30–002-CI), 2 mmol/L L-glutamine (cat. no. 25–005-CI), and 0.01 M HEPES buffer (cat. no. 25–060-CI) (all supplied by Corning, Manassas, VA, USA). Cultures were maintained at 37 °C in a humidified environment with 5 % CO_2. Cells were plated in 96-well plates at a density of 3×10^3 cells per well and allowed to adhere overnight. Subsequently, compound **12** was administered at concentrations of 5, 10, 15, 30, 100, and 128 μg/mL, with exposure times of 24 and 48 h. After treatment, 100 μL of MTT solution (3-(4,5-dimethylthiazol-2-yl)-2,5-diphenyltetrazolium bromide; Merck, Italy; cat. no. M5655) was added per well at a final concentration of 0.25 mg/mL in DMEM and incubated for 3 h at 37 °C. The resulting formazan crystals were dissolved in 100 μL of DMSO, and absorbance was recorded at 540 nm using a Thermo Scientific Multiskan GO plate reader (Thermo Fisher Scientific, Waltham, MA, USA).

The results are expressed as mean ± SEM of $n = 3$ experiments. The data were analyzed using GraphPad Prism 5.0 software (San Diego, CA, USA). Statistical significance was assessed using one-way ANOVA.

3. Results and discussion

3.1. Phytochemical analysis of hydroalcoholic extract

Ruscus spp. are a rich source of steroidal saponins that can be classified in two classes: pentacyclic furostanol saponins featuring a hemiketal function at C-22 and a glucose unit at C-26, and hexacyclic spirostanol saponins featuring a ketal at C-22. Both classes have a variable number of sugar residues at different positions of the aglycone, the most common of which are arabinose, rhamnose and glucose [2]. In our study, the hydroalcoholic extract obtained from rhizomes and roots of *Ruscus aculeatus* was subjected to extraction and chromatographic analyses.

In particular, the dry extract (33 g), subjected to a modified Kupchan's partitioning procedure [13], was dissolved in MeOH:H_2O containing 10 % H_2O and partitioned against n-hexane (3 × 800 mL) to give 200 mg of the crude hexanic extract. The water content (% *v*/v) was adjusted to 30 % and partitioned against $CHCl_3$, to give 3.6 g of crude extract. The aqueous phase was concentrated to remove MeOH and then extracted with *n*-BuOH yielding 19.2 g of glassy material. 2 g of $CHCl_3$ extract was then subjected to a droplet counter-current chromatography (DCCC) using $CHCl_3$/MeOH/H_2O (7:13:8) in the ascending mode (the lower phase was the stationary phase), flow rate 7 mL/min.

Fractions were monitored by TLC on SiO_2 with $CHCl_3$/MeOH/H_2O (80:18:2) as eluent and combined on the basis of their similar TLC retention factors, obtaining 12 fractions.

Purification of the $CHCl_3$ fractions 2–5, 7 and 9 by HPLC on a Nucleodur 100–5 C18 column (5 μm, 4.6 mm i.d x 250 mm; flow rate 1

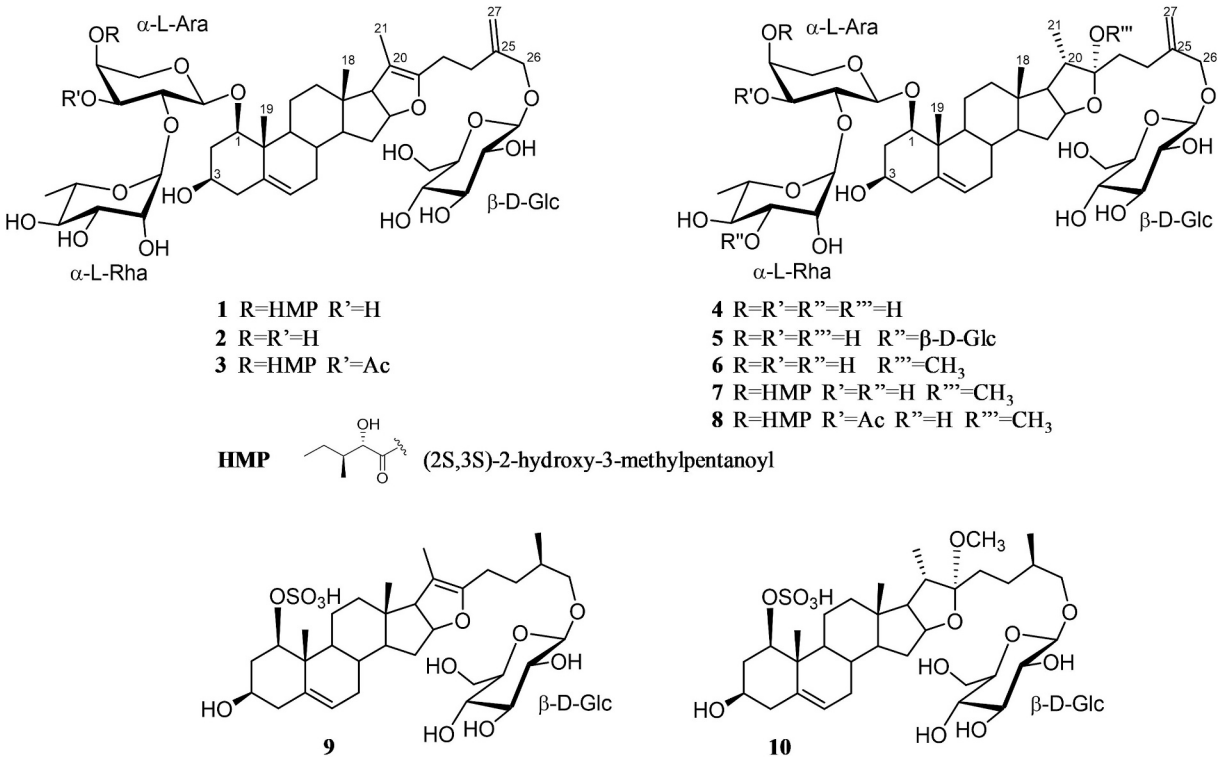

Fig. 1. New compound (**1**), known furostanol saponins (**2**–**8**) and sulphated furostanol saponins (**9**, **10**) isolated in this study.

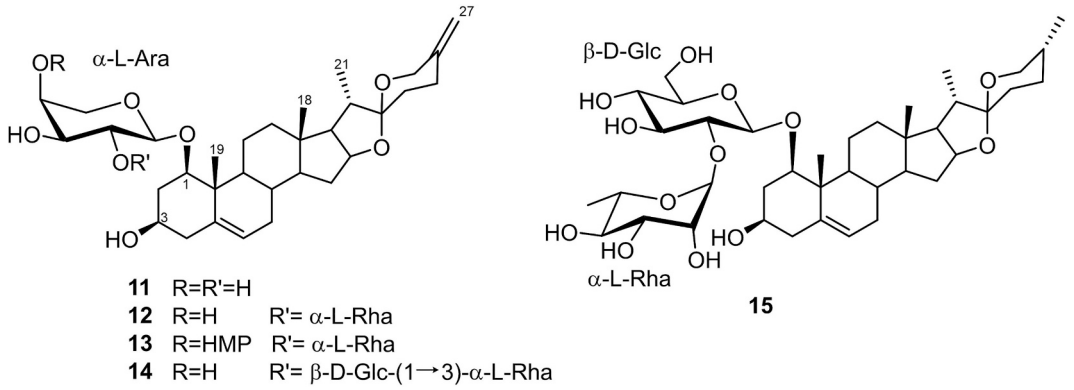

Fig. 2. Known spirostanol saponins (**11**–**15**) isolated in this study.

mL/min) gave the pure compounds **1**–**4**, **7**, **8**, **11**, **12**, **14** and **15** (Figs. 1 and 2).

The *n*-BuOH extract (2.0 g) was submitted to DCCC with *n*-BuOH/Me_2CO/H_2O (3:1:5) in the descending mode (the upper phase was the stationary phase). The obtained fractions were monitored by TLC on Silica gel plates with *n*-BuOH/AcOH/H_2O (12:3:5) and $CHCl_3$/MeOH/H_2O (80:18:2) as eluents.

Six fractions A-E were obtained and purified by HPLC on a Nucleodur 100–5 C18 column (5 μm, 4.6 mm i.d x 250 mm; flow rate 1 mL/min) to give the pure compounds **5**, **6**, **9**, **10** and **13** (Figs. 1 and 2).

The furostanol saponins share as a common structural feature a double bond at C-25-C-27 positions and differ each other for the presence of a $\Delta^{20(22)}$ unsaturation (**1**–**3**) or for a hydroxy (**4**–**5**) or methoxy (**6**–**8**) group at C-22.

Additionally, the arabinose unit often bears a (2*S*,3*S*)-2-hydroxy-3-methylpentanoyl moiety (HMP) at C-4 or/and an acetyl group at C-3 such as in compounds **1**, **3**, **7** and **8**. (Fig. 1).

Compound **6** is the 22-methoxyfurostanol analogue of compound **4**, which we previously isolated in 2012 [22]. The presence of the methoxy group was supported by ^{1}H NMR and ^{13}C NMR signals.

As reported in literature, compounds **6**–**8** and **10** may be considered artefacts of the extraction and isolation procedure, since interconversion between 22-hydroxy and 22-methoxy furostanol oligosides is known to occur [22,29,30].

The spirostanol saponins **11**–**15** (Fig. 2) are characterized by the presence of the typical spiroketal system in the aglycone moiety. These compounds differ mainly in their sugar chain composition and substitution pattern. Notably, compound **12** emerged as the major metabolite from the $CHCl_3$ extract.

Structural elucidation of all isolated compounds was performed by NMR spectroscopic analysis (1D and 2D experiments), mass spectrometric data (ESI-MS) and comparison with previously reported literature values.

Compound **1**, the only novel metabolites identified, showed a pseudomolecular ion peak at *m/z* 981.5 $[M-H]^-$ in the negative ESI-MS spectrum. Significant fragment ion was observed at *m/z* 867,

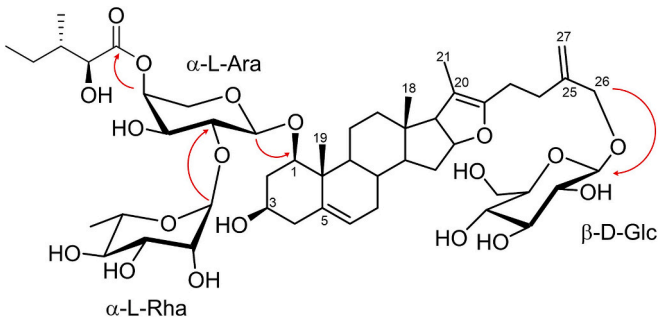

Fig. 3. Key HMBC correlations for new compound **1.**

corresponding to the loss of a 2-hydroxy-3-methylpentanoyl (HMP) unit, and *m/z* 721 resulting from combined loss of the HMP group and a deoxyhexose unit.

The ^{1}H NMR spectrum of the aglycone portion revealed signals for three tertiary methyl groups at δ_H 1.61 (s), 1.10 (s) and 0.72 (s), an exomethylene group at δ_H 5.09 (br s) and 4.93 (br s), and an olefinic proton at δ_H 5.56 (br d, $J = 5.7$ Hz).

Additionally, an AB system at δ_H 4.33 and 4.11 (each 1H, d, $J = 12.6$ Hz) revealed the presence of an isolated oxygenated methylene.

A detailed interpretation of HSQC and HMBC correlations supported the presence of a furostanol-type skeleton in compound **1** [15] (Table 1). In particular, we disclosed the presence of two oxygenated methines (CH-1 at δ_H 3.39 and δ_C 84.1 and CH-3 at δ_H 3.35 and δ_C 69.2), an oxygenated methine of the tetrahydrofuran ring (CH-16 at δ_H 4.70 and δ_C 85.7). The presence of two quaternary olefinic carbons at δ_C 152.1 and 105.2 and the downfield shift of the methyl group at C-21, suggested the replacement of the C-22 hemiketal moiety [20] with a $\Delta^{20(22)}$ double bond.

This structural feature was confirmed based on key HMBC correlations between the Me-21 (δ_H 1.61) and C-20 (δ_C 105.2) and C-22 (δ_C 152.1). In addition to the signals of the aglycone, the ^{1}H NMR spectrum showed signals which suggested the presence of a (2*S*,3*S*)-2-hydroxy-3-methylpentanoyl unit (HMP), often found in saponins isolated from *Ruscus*. In particular, in the ^{1}H NMR spectrum we observed two methyl groups at δ_H 1.01 (d, $J = 6.8$ Hz) and 0.95 (t, $J = 7.5$ Hz), a methylene at δ_H 1.64 (m) and 1.30 (m), a methine at δ_H 1.88 (m), a hydroxy methine at δ_H 4.07 (d, $J = 12.8$ Hz) and in the ^{13}C NMR spectrum a carbonyl ester at δ_C 179.8. As concerning the saccharide portion, the ^{1}H NMR spectrum showed signals for three anomeric protons at δ_H 4.33 (d, $J = 7.7$ Hz), 5.29 (br d, $J = 1.3$ Hz) and 4.27 (d, $J = 7.8$ Hz), which were correlated in the HSQC spectrum with the anomeric carbons at δ_C 100.5, 101.1 and 102.6 respectively. The three sugar units were identified as β-D-glucopyranose (Glc), α-L-arabinopyranose (Ara) and α-L-rhamnopyranose (Rha), after the acidic hydrolysis of **1** and GC analysis. The assignment of all proton and carbon chemical shifts of the sugar moieties was performed through a detailed analysis of 2D NMR spectra (COSY, HMBC and HSQC) (Table 1).

The glycosidic linkages were deduced based on characteristic glycosylation-induced carbon shifts observed at C-1 and C-26 of the aglycone (δ_C 84.1 and 72.7, respectively) and C-2 and C-4 of the arabinose unit (δ_C 75.3 and 74.1, respectively), as well as through key HMBC cross-peaks. Specifically, long-range correlations were observed between H-1ara and C-1agly, H-26agly and C-1glc, H-1rha and C-2ara, and H-4ara and C-1HMP (Fig. 3).

Based on these data, compound **1** was identified as 26-O-β-D-glucopyranosyl-furosta-5,20(22),25(27)-triene-1β,3β,26-triol 1-O-α-L-rhamnopyranosyl-(1 → 2)-4-[(2*S*,3*S*)-2-hydroxy-3-methylpentanoyl]-α-L-arabinopyranoside.

Table 2
In vitro antimicrobial activity for $CHCl_3$ extract, and compounds **11**, **12**, **12a** and **14**. The number in bracket showed the percentage of cell growth reduction.

Compounds	*S. aureus* ATCC 29213	*S. aureus* ATCC 43300	*E. coli* ATCC 25922	*C. albicans* ATCC 10231
$CHCl_3$ Extract	128 (20 %)	128 (25 %)	>128	128 (20 %)
11	>128	>128	>128	>128
12	128 (30 %)	128 (36 %)	>128	64 (31 %)
12a	>128	>128	>128	>128
14	>128	>128	>128	>128
DMSO	>128	>128	>128	>128
VAN	2	2	ND	ND
OXA	2	≥2 (R)	ND	ND
TOB	ND	ND	2	ND
AMB	ND	ND	ND	2
VRC	ND	ND	ND	≥0,12 (R)

Conventional OXA (oxacillin), VRC (voriconazole), VAN (vancomycin), TOB (tobramycin) and AMB (amphotericin B) were used as positive control of antimicrobial activity. Concentrations reported μg/mL.

3.2. Antimicrobial activity evaluation

The medicinal properties of *Ruscus aculeatus* extract, particularly vasoprotective, anti-inflammatory, and venotonic effects, are well-documented in literature [1–3]. Several studies have also reported antimicrobial activity of its aqueous and hydroethanolic extracts against multidrug-resistant bacteria [30], and fungi [10]. However, the antimicrobial potential of its individual components has remained poorly understood. This study focuses on deglucoruscin (**12**) (also known as ruscoponticoside C), a spirostanol glycoside and identified in this study as the major compound in *R. aculeatus* hydroalcholic extract. While deglucoruscin (**12**) is believed to play a key role in the extract's vascular and anti-inflammatory effects [25]—such as improving venous tone and lymphatic drainage—its specific contribution to antimicrobial activity has never been directly investigated.

Given the urgent global health threat posed by antimicrobial resistance (AMR), the search for new agents, including plant-derived compounds, is critical. Deglucoruscin (**12**) may offer antimicrobial properties on its own or act synergistically with conventional drugs. This study aims to fill the current knowledge gap by evaluating, for the first time, the antimicrobial activity of isolated deglucoruscin (**12**), with the goal of better understanding its potential therapeutic role and its relevance in combating resistant infections.

Resistance leads to longer and more severe illnesses, higher risk of transmission, and reliance on more expensive or toxic second- and third-line treatments.

Deglucoruscin (**12**) exhibited only modest standalone antimicrobial activity but showed strong synergistic effects when combined with conventional drugs.

This is especially useful in treating tough or resistant infections like those caused by *Candida albicans* and *Staphylococcus aureus*. In clinical settings, synergistic drug combinations improve effectiveness, lower drug doses, reduce toxicity, and help prevent resistance [26]. Understanding and applying synergism is essential for optimizing antimicrobial therapy and improving patient out-comes. The $CHCl_3$ extract of *Ruscus aculeatus* was evaluated for its antimicrobial activity against two Gram positive strains of *S. aureus* ATCC 29213 and *S. aureus* ATCC 43300, one Gram-negative strain of *E. coli* ATCC 25922, and the yeast *C. albicans* ATCC 10231, showing a mild activity against both strains of *S. aureus* and *C. albicans* (Table 2).

Therefore, we investigated whether the major component (**12**) of the $CHCl_3$ extract of *Ruscus* was responsible for the observed activity, also evaluating the activity of its closely related derivatives, such as compounds **11** and **14**, bearing respectively one or three sugar units, as well as the corresponding aglycone (**12a**), obtained by acidic hydrolysis. Only compounds **12** showed a weak activity, reducing of about 30 % the growth of *S. aureus* ATCC 29213, and 36 % the growth *S. aureus* ATCC

Table 3
Synergistic activity of compound **12** in combination with standard drugs.

Strains	Compound 12 concentration	Drug	Drug MIC	FIC Index	Interaction
S. aureus **ATCC 43300**	32	OXA (0.5)	10	0.3	Synergistic
C. albicans **ATCC 10231**	4	VRC (0.125)	30	0.035	Strongly synergistic

OXA = oxacillin; VRC = voriconazole; MIC = minimum inhibitory concentration; FIC = fractional inhibitory concentration index. Concentrations reported μg/mL.

43300 at a concentration of 128 μg/mL. Similarly, compound **12** reduced by 31 % the growth of *C. albicans* strain at 64 μg/mL. None of the compounds were effective against *E. coli* (Table 2).

To test the ability of compound **12** to work in combination with oxacillin (OXA) or voriconazole (VRC), antimicrobial synergy studies were performed by applying the checkerboard method (Table 3). This assay is used to determine the impact of the combination of antimicrobics on their potency in comparison to their individual activities. The Fractional Inhibitory Concentration (FIC) index value considers the combination of antibiotics that produces the greatest change from the individual antibiotic's MIC. Oxacillin was tested in association with compound **12**, against *S. aureus* ATCC 43300, using different concentrations of both compounds. A complete absence of growth was observed only when compound **12** at 32 μg/mL was combined with OXA at 0.5 μg/mL, whose MIC is 10 μg/mL on *S. aureus* ATCC 43300. The FIC index value of 0.3 suggested a synergistic interaction between compound **12** and OXA. The same assay was performed to test the synergistic interaction of compound **12** with VRC. A complete absence of *C. albicans* growth was observed when compound **12** at 4 μg/mL was combined with VRC at 0.125 μg/mL, whose MIC is 30 μg/mL.

The FIC index value of 0.035 suggested a strong synergistic interaction between compound **12** and VRC. Finally, we tested the bacteriostatic or fungistatic activity of the synergistic drug combinations.

We observed bacteriostatic or fungistatic activity in both combinations. This result is of strong interest since antibiotics can cause a selective pressure by killing susceptible microorganisms, allowing antibiotic-resistant bacteria or yeasts to survive. By completely or partially inhibiting the growth of wild-type microorganisms, antibiotics cause a selective pressure that will increase the prevalence of resistance. HaCaT keratinocytes were used as human *in vitro* model to evaluate the cytotoxic properties of compound **12**.

The results showed that compound **12** was not cytotoxic at the concentrations used in the checkerboard assay ($\leq$ 20 μg/mL) that were effective in reducing the MIC of voriconazole against *Candida albicans* ATCC 10231. Conversely, at higher concentrations ($\geq$ 30 μg/mL), compound **12** exhibited cytotoxic activity on HaCaT cell line (IC_{50} 32.3 μg/mL at 24 h and 27.6 μg/mL at 48 h), falling within the range of its anti-*MRSA* activity (Fig. 4).

To the best of our knowledge, this is the first study reporting a synergistic effect of deglucoruscin (**12**). In a previous work, we demonstrated that this molecule targets the F_0F_1-ATP synthase, a key enzyme in cellular energy production [24]. Inhibition of ATP synthesis can induce a severe energy crisis in *Candida albicans*, thereby potentiating the activity of voriconazole.

Under these conditions, the pathogen would be simultaneously deprived of the ATP required for essential repair mechanisms, stress response pathways, and survival processes, ultimately resulting in more rapid and effective cell death. The synergistic interaction observed between deglucoruscin and voriconazole against *Candida albicans* is a key finding of this study opening the way to further investigations.

4. Conclusions

This study provides the first direct evidence that deglucoruscin (**12**), a known spirostanol saponin and the main metabolite in the $CHCl_3$ extract of *Ruscus aculeatus*, is responsible for the synergistic antimicrobial effects previously attributed to the plant's crude extracts. Deglucoruscin alone exhibited modest inhibitory activity against *S. aureus* and *C. albicans*; however, when combined with standard drugs-oxacillin (OXA) or voriconazole (VRC) it significantly reduced the MIC values of both drugs against resistant strains. These synergistic effects occurred at non-cytotoxic concentrations, supporting the potential of deglucoruscin as a safe and effective adjuvant in antimicrobial therapy.

Importantly, the concentration of compound **12** used in this synergistic combination falls below the cytotoxic threshold, as confirmed by MTT assay, highlighting its potential safety for therapeutic application. In addition to this biological insight, the study also led to the isolation and full structural characterization of a new furostanol saponin (compound **1**), enriching the phytochemical profile of *R. aculeatus*.

Together, these findings not only validate the traditional medicinal use of *Ruscus aculeatus* but also open new avenues for the development of plant-derived molecules to combat antimicrobial resistance. This work represents a valuable contribution to natural product research and supports further exploration of deglucoruscin and related saponins as resistance-modifying agents.

CRediT authorship contribution statement

Carmen Festa: Writing – original draft, Investigation. **Claudia Finamore:** Validation, Investigation. **Mattia Cammarota:** Validation, Investigation. **Elisabetta Panza:** Validation, Investigation. **Silvia Marchianò:** Validation, Investigation. **Stefano Fiorucci:** Supervision. **Angela Zampella:** Supervision. **Elisabetta Buommino:** Validation, Investigation, Conceptualization. **Simona De Marino:** Writing – review & editing, Supervision, Funding acquisition, Conceptualization.

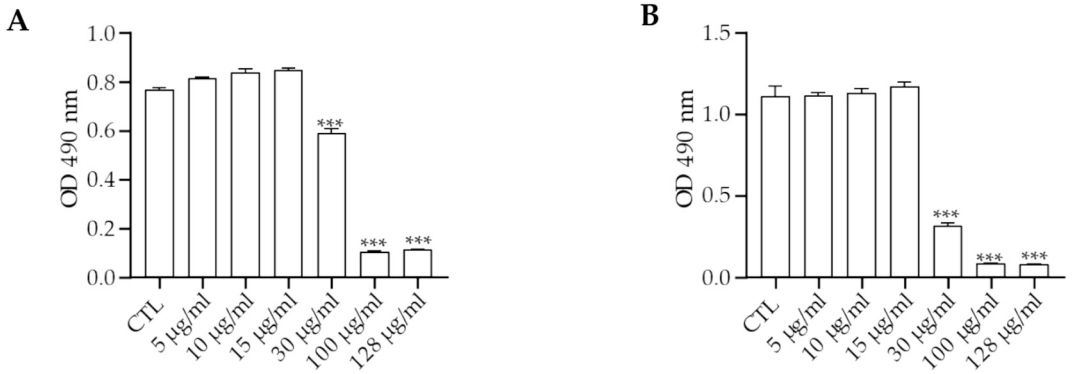

Fig. 4. MTT assay on HaCaT cell lines treated with compound **12** following 24 h and 48 h (A and B, respectively) of incubation.

Funding

This work was supported by the E.U "Next Generation EU" by the PRIN 2022 framework (Project n°: 2022MPTT35) "Production and characterization of new bioactive molecules against emerging and/or multidrug-resistant pathogens by neglected poly-extremophilic marine fungi (MYCOSEAS).

Declaration of competing interest

The authors declare no conflicts of interest.

Acknowledgments

We thank Dr. Chiara Cassiano for her support with the mass spectrometry (MS) analyses, which were performed at the Analisi Strumentale Laboratory of the Department of Pharmacy, University of Naples Federico II.

We are also grateful to Claudia Pietranico and Filomena Librera for the technical support to the microbiological assays.

We also gratefully acknowledge Indena S.p.A. for kindly providing the hydroalcoholic extract of *Ruscus aculeatus*, which was essential for this study.

Appendix A. Supplementary data

Supplementary data to this article can be found online at https://doi.org/10.1016/j.fitote.2025.106895.

Data availability

All relevant data are included within the article and its Supplementary Materials.

References

[1] P.A. Thomas, T.A. Mukassabi, Biological flora of the British Isles: *Ruscus aculeatus*, J. Ecol. 102 (2014) 1083–1100, https://doi.org/10.1111/1365-2745.12265.
[2] M. Masullo, C. Pizza, S. Piacente, *Ruscus* genus: a rich source of bioactive steroidal saponins, Planta Med. 82 (2016) 1513–1524, https://doi.org/10.1055/s-0042-119728.
[3] E. Bouskela, F.Z. Cyrino, G. Marcelon, Effects of *Ruscus* extract on the internal diameter of arterioles and venules of the hamster cheek pouch microcirculation, J. Cardiovasc. Pharmacol. 22 (1993) 221–224, https://doi.org/10.1097/00005344-199308000-00008.
[4] E. Bouskela, F.Z. Cyrino, G. Marcelon, Inhibitory effect of the *Ruscus* extract and of the flavonoid hesperidine methylchalcone on increased microvascular permeability induced by various agents in the hamster cheek pouch, J. Cardiovasc. Pharmacol. 22 (1993) 225–230, https://doi.org/10.1097/00005344-199308000-00009.
[5] R. Nocera, D. Eletto, V. Santoro, V. Parisi, M.L. Bellone, M. Izzo, A. Tosco, F. Dal Piaz, G. Donadio, N. De Tommasi, Design of an herbal preparation composed by a combination of *Ruscus aculeatus* L. and *Vitis vinifera* L. extracts, magnolol and diosmetin to address chronic venous diseases through an anti-inflammatory effect and AP-1 modulation, Plants 12 (2023) 1051, https://doi.org/10.3390/plants12051051.
[6] G. Ozer, E. Guzelmeric, G. Sezgin, E. Ozyurek, A. Arslan, E. Sezik, E. Yesilada, Comparative determination of ruscogenins content in butcher's broom rhizome samples gathered from the populations grownin differents oil conditions in the Marmara Region and attempts for pilot field cultivation of rhizomes, J. Chem. Metrol. 12 (2018) 78–88, https://doi.org/10.25135/jcm.17.18.05.094.
[7] L. Chakuleska, R. Michailova, A. Shkondrov, V. Manov, N. Zlateva-Panayotova, G. Marinov, R. Petrova, M. Atanasova, I. Krasteva, N. Danchev, I. Doytchinova, Bone protective effects of purified extractfrom *Ruscus aculeatus* on ovariectomy-induced osteoporosis in rats, Food Chem. Toxicol. 132 (2019) 110668, https://doi.org/10.1016/j.fct.2019.110668.
[8] G. Balica, O. Vostinaru, M. Tamas, G. Crisan, C. Mogosan, Anti-inflammatory effect of the crude steroidal saponin from the rhizomes of *Ruscus aculeatus* L. (Ruscaceae) in two rat models of acute inflammation, J Food Agric Environ 11 (2013) 106–108.
[9] N. Hadžifejzović, J. Kukić-Marković, S. Petrović, M. Soković, J. Glamočlija, D. Stojković, A. Nahrstedt, Bioactivity of the extracts and compounds of *Ruscus aculeatus* L. and *Ruscus hypoglossum* L, Ind. Crop. Prod. 49 (2013) 407–411, https://doi.org/10.1016/j.indcrop.2013.05.036.
[10] B. Renga, C. Festa, S. De Marino, S. Di Micco, M.V. D'Auria, G. Bifulco, S. Fiorucci, A. Zampella, Molecular decodification of gymnemic acids from *Gymnema sylvestre*. Discovery of a new class of liver X receptor antagonists, Steroids 96 (2015) 121–131, https://doi.org/10.1016/j.steroids.2015.01.024.
[11] C. Finamore, C. Festa, M. Cammarota, L. Spinelli, E. Morretta, C. Cassiano, M. C. Monti, S. Marchianò, C. Massa, F. Moraca, A. Lupia, B. Catalanotti, S. Fiorucci, A. Zampella, S. De Marino, Exploring *Boswellia serrata* triterpenes: a new frontier in leukemia inhibitory factor receptor modulation, ACS Omega 10 (2025) 22269–22284, https://doi.org/10.1021/acsomega.5c03492.
[12] S.M. Kupchan, R.W. Britton, M.F. Ziegler, C.W. Sigel, Bruceantin, a new potent antileukemic simaroubolide from Brucea antidysenterica, J. Organomet. Chem. 38 (1973), https://doi.org/10.1021/jo00941a049, 178–17.
[13] Y. Mimaki, Y. Takaashi, M. Kuroda, Y. Sashida, T. Nikaido, Steroidal saponins from *Nolina recurvata* stems and their inhibitory activity on cyclic AMP phosphodiesterase, Phytochemistry 42 (1996) 1609–1615, https://doi.org/10.1016/0031-9422(96)00107-0.
[14] A. Skhirtladze, A. Plaza, P. Montoro, M. Benidze, E. Kemertelidze, C. Pizza, S. Piacente, Furostanol saponins from *Yucca gloriosa* L. rhizomes, Biochem. Syst. Ecol. 34 (2006) 809–814, https://doi.org/10.1016/j.bse.2006.04.008.
[15] T. Muzashvili, A. Perrone, A. Napolitano, E. Kemertelidze, C. Pizza, S. Piacente, Caucasicosides E-M, furostanol glycosides from *Helleborus caucasicus*, Phytochemistry 72 (2011) 2180–2188, https://doi.org/10.1016/j.phytochem.2011.08.008.
[16] A. Di Lazzaro, A. Morana, C. Schiraldi, A. Martino, C. Ponzone, M. De Rosa, An enzymatic process for the production of the pharmacologically active glycoside desglucodesrhamnoruscin from *Ruscus aculeatus* L, J. Mol. Catal. B Enzym. 11 (2001) 307–314, https://doi.org/10.1016/S1381-1177(00)00152-1.
[17] E. de Combarieu, M. Falzoni, N. Fuzzati, F. Gattesco, A. Giori, M. Lovati, R. Pace, Identification of *Ruscus* steroidal saponins by HPLC-MS analysis, Fitoterapia 73 (2002) 583–596, https://doi.org/10.1016/s0367-326x(02)00220-4.
[18] Y. Mimaki, M. Kuroda, A. Kameyama, A. Yokosuka, Y. Sashida, New steroidal constituents of the underground parts of *Ruscus aculeatus* and their cytostatic activity on HL-60 cells, Chem. Pharm. Bull. 46 (1998) 298–303, https://doi.org/10.1248/cpb.46.298.
[19] A. Mari, A. Napolitano, A. Perrone, C. Pizza, S. Piacente, An analytical approach to profile steroidal saponins in food supplements: the case of *Ruscus aculeatus*, Food Chem. 134 (2012) 461–468, https://doi.org/10.1016/j.foodchem.2012.02.099.
[20] G.V. Shevchuk, Yu.S. Vollerner, A.S. Shashkov, M.B. Gorovits, V.Ya. Chirva, Steroids of the spirostan and furostan series from *Nolina microcarpa*. III. Structure of nolinofurosides G and H, Khimiya Prirodnykh Soedinenii 6 (1991) 801–806, https://doi.org/10.1007/BF00630361.
[21] S. De Marino, C. Festa, F. Zollo, M. Iorizzi, Novel steroidal components from the underground parts of *Ruscus aculeatus* L, Molecules 17 (2012) 14002–14014, https://doi.org/10.3390/molecules171214002.
[22] E. Bombardelli, A. Bonati, B. Gabetta, G. Mustich, Glycosides from rhizomes of *Ruscus aculeatus*, Fitoterapia 42 (1971) 127–136.
[23] F. Del Gaudio, C. Festa, M. Mozzicafreddo, M. Vasaturo, A. Casapullo, S. De Marino, R. Riccio, M.C. Monti, Biomolecular proteomics discloses ATP synthase as the main target of the natural glycoside deglucoruscin, Mol. BioSyst. 12 (2016) 3132–3138, https://doi.org/10.1039/c6mb00460a.
[24] M. Barbić, E.A. Willer, M. Rothenhöfer, J. Heilmann, R. Fürst, G. Jürgenliemk, Spirostanol saponins and esculin from *Rusci* rhizoma reduce the thrombin-induced hyperpermeability of endothelial cells, Phytochemistry 90 (2013) 106–113, https://doi.org/10.1016/j.phytochem.2013.02.004.
[25] L. Tang, Z. Wang, H. Wu, A. Yokosuka, Y. Mimaki, Steroidal glycosides from the underground parts of *Dracaena thalioides* and their cytotoxic activity, Phytochemistry 107 (2014) 102–110, https://doi.org/10.1016/j.phytochem.2014.07.021.
[26] E. Buommino, S. De Marino, M. Sciarretta, M. Piccolo, C. Festa, M.V. D'Auria, Synergism of a novel 1,2,4-oxadiazole-containing derivative with oxacillin against methicillin-resistant *Staphylococcus aureus*, Antibiotics 10 (2021) 1258, https://doi.org/10.3390/antibiotics10101258.
[27] S.K. Pillai, R.C. Moellering, G.M. Eliopoulos, Antimicrobial combinations, in: V. Lorian (Ed.), Antibiotics in Laboratory Medicine, fifth ed., the Lippincott Williams & Wilkins Co, Philadelphia, , pp. 365–440.
[28] S. Rosselli, A. Maggio, M. Bruno, V. Spadaro, C. Formisano, C. Irace, C. Maffettone, N. Mascolo, Furostanol saponins and ecdysones with cytotoxic activity from *Helleborus bocconei* ssp. intermedius, Phytother. Res. 23 (2009) 1243–1249, https://doi.org/10.1002/ptr.2569.
[29] A. Debella, E. Haslinger, O. Kunert, G. Michl, D. Abebe, Steroidal saponins from *Asparagus africanus*, Phytochemistry 51 (1999) 1069–1075, https://doi.org/10.1016/s0031-9422(99)00051-5.
[30] J.P.B. Rodrigues, Â. Fernandes, M.I. Dias, C. Pereira, T.C.S.P. Pires, R.C. Calhelha, A.M. Car-valho, I.C.F.R. Ferreira, L. Barros, Phenolic compounds and bioactive properties of *Ruscus aculeatus* L. (Asparagaceae): the pharmacological potential of an underexploited subshrub, Molecules 26 (2021) 1882, https://doi.org/10.3390/molecules26071882.